WILEY-VCH

Identification of Individual Exosome-Like Vesicles by Surface Enhanced Raman Spectroscopy

*Stephan Stremersch, Monica Marro, Bat-El Pinchasik, Pieter Baatsen, An Hendrix, Stefaan C. De Smedt, Pablo Loza-Alvarez, Andre G. Skirtach, Koen Raemdonck, Kevin Braeckmans**

MSc. S. Stremersch, Prof. S. C. De Smedt, Dr. K. Raemdonck
Laboratory of General Biochemistry and Physical Pharmacy, Faculty of Pharmaceutical Sciences, Ghent University, Ottergemsesteenweg 460, 9000 Ghent, Belgium

Dr. M. Marro, Prof. P. Loza-Alvarez
ICFO-Institut de Ciencies Fotoniques, The Barcelona Institute of Science and Technology, Av. Carl Friedrich Gauss 3, 08860 Castelldefels (Barcelona), Spain

Dr. B. Pinchasik,
Department of Interfaces, Department of Biomaterials, Max Planck Institute of Colloids and Interfaces, Am Mühlenberg 1 OT Golm, 14476 Potsdam, Germany

Dr. P. Baatsen
EM-facility EMoNe, VIB-KULeuven Bio Imaging Core and Center for Human Genetics, KULeuven, Herestraat 49,3000 Leuven, Belgium

Dr. A. Hendrix
Department of Radiation Oncology and Experimental Cancer Research, Laboratory of Experimental Cancer Research, Ghent University Hospital, De Pintelaan 185, 900 Ghent, Belgium

Prof. A. G. Skirtach
Department of Molecular Biotechnology, Ghent University, Coupure Links 653, 9000 Ghent, Belgium
Department of Interfaces, Department of Biomaterials, Max Planck Institute of Colloids and Interfaces, Am Mühlenberg 1 OT Golm, 14476 Potsdam, Germany
Centre for Nano- and Biophotonics, Ghent University, Ghent, Belgium

Prof. K. Braeckmans*
Department of Pharmaceutics
Faculty of Pharmaceutical Sciences, Ghent University
Ottergemsesteenweg 460, 9000 Ghent
Belgium
Tel.: +32 9 264 80 98
Email: kevin.Braeckmans@ugent.be
Centre for Nano- and Biophotonics, Ghent University, Ghent, Belgium

Keywords: exosome-like vesicles, gold nanoparticles, surface enhanced Raman spectroscopy, multivariate statistical analysis, diagnostics

Exosome-like vesicles (ELVs) are a novel class of biomarkers that are receiving a lot of attention for the detection of cancer in an early stage. In this study the feasibility of using a Surface Enhanced Raman Spectroscopy (SERS) based method to distinguish between ELVs derived from different cellular origins is evaluated. A gold nanoparticle based shell is deposited on the surface of ELVs derived from cancerous and healthy cells which enhances the Raman signal while maintaining a colloidal suspension of individual vesicles. This nano-coating allows the recording of SERS spectra from single vesicles. By using Partial Least Square Discriminative Analysis (PLS-DA) on the obtained spectra, vesicles from different origin can be distinguished, even when present in the same mixture. This proof-of-concept study paves the way for non-invasive (cancer) diagnostic tools based on exosomal SERS fingerprinting in combination with multivariate statistical analysis.

1. Introduction

To maximize the impact of current cancer treatments it is essential to detect carcinogenic cells in an early stage. To this end, the discovery of sufficiently sensitive and specific biomarkers is of foremost importance. Recently, circulating extracellular vesicles (EVs), especially exosomes, have emerged as a potential new class of biomarkers for early detection and treatment monitoring in cancer and other diseases.[1, 2]

Exosomes are small (40-200 nm in diameter) membranous vesicles actively released by cells. They are composed of a protein-lipid bilayer encapsulating an aqueous core comprising nucleic acids and soluble proteins. Exosomes typically originate from the endosomal pathway. By inward budding of late endosomes, multivesicular bodies are formed which then fuse with the limiting membrane of the cell concomitantly releasing the exosomes.[3] This mechanism allows the cell to discard waste material[4, 5] and is associated with intercellular communication.[6, 7]

Exosomes are of interest for diagnostic and prognostic applications as they contain molecules derived directly from the parent cell.[8] In addition, they are fairly easily accessible as they are found in various body fluids (e.g. blood, salvia, urine, breast milk, ascites, etc.).[9-11] Currently, most exosome based diagnostic approaches focus on identifying specific molecular components by elaborate 'omics' studies.[12] Examples are elevated levels of miR-21 in exosomes of hepatocellular cancer patients[13] and the presence of EGFRvIII mutant proteins on exosomes derived from a specific glioblastoma subtype.[14] Despite the fact that these techniques provide detailed information on the molecular composition of exosomes, they rely on complicated and time-consuming protocols. Moreover, these analyses are performed on the overall EV population level which makes it less likely to find low abundant subpopulations. Indeed, considering that most cells secrete EVs as part of their normal function, it is to be expected that the amount of vesicles derived from diseased cells is comparatively low. Accordingly, the detection of altered levels of low abundant components in a bulk analysis is quite challenging. Furthermore, it is becoming apparent that one cell type may release multiple subtypes of EVs due to which bulk analysis is prone to missing specific subtypes or subtype ratios of vesicles.[15-17] Therefore, techniques capable of identifying individual exosomes could prove very valuable, but are currently lacking.

In this manuscript, a new approach is explored for single exosome identification based on surface enhanced Raman spectroscopy (SERS) for diagnostic applications. Raman spectroscopy is a label-free technique based on inelastic scattering of laser light due to interaction of photons with molecular vibrations. As such, the Raman spectrum of inelastically scattered photons contains information on the molecular composition of the sample. Raman spectroscopy has been used before to characterize EVs.[18, 19] However, as it is a very inefficient process (only 1 in 10^{6-8} photons is scattered inelastically), a high sample concentration is required in combination with high laser

power and long signal integration times. High throughput screening of single vesicles by Raman spectroscopy is therefore not feasible.[20]

Fortunately, the Raman signal can be strongly enhanced (up to $10^{14\text{-}15}$ times) by using SERS.[21] SERS is based on the enhancement of the incident and scattered electromagnetic field by plasmon excitation on irregular (metal) surfaces, typically composed of Au or Ag.[22-24] As it has single molecule sensitivity, SERS is increasingly applied for the characterization of biological samples.[25, 26] In this respect, different types of SERS-substrates have been developed to obtain plasmon enhancement and record Raman spectra from (sub)cellular components down to the single biomolecule level.[27] These can be, but are not limited to, well defined nanostructured surfaces of gold[28] or silver[29] and (intracellular) aggregated Ag[30] or AuNP[31]. Both Ag-nanograin coated chips and precipitated AuNP clusters were recently applied for bulk EV measurements.[32, 33] These few reports show the feasibility of obtaining SERS spectra from an EV sample and the capability to differentiate between EVs from different origin.[32, 33] However, it is important to note that these previous analyses were still performed on bulk vesicles from a single cell type. Yet, clinical samples contain EVs from different origin in a mixture, hampering the further implementation of bulk Raman measurements for diagnostic applications.

To enable true single vesicle SERS identification, here we demonstrate to the best of our knowledge for the first time, that EVs can be functionalized with gold nanoparticles (AuNP) on their surface, forming an irregularly shaped nanoshell that enables the generation of an enhanced Raman signal while maintaining a colloidal suspension of individual vesicles. As proof-of-concept of the diagnostic potential of this approach, we show that vesicles derived from B16F10 melanoma cells can be successfully identified and quantified in a mixture with red blood cell (RBC)-derived vesicles.

2. Results

2.1. Exosome-like vesicle (ELV) purification and characterization

The potential of SERS to distinguish between vesicles released by two distinct cell types was explored using ELVs from RBC and B16F10 melanoma cancer cells. The terminology ELVs is further used throughout the manuscript as it is to date impossible to conclusively claim that all purified vesicles are originating from the endosomal cell compartment and consequently can be termed exosomes.[34] To this end, it is more appropriate to use the term ELVs. B16F10 cells were cultured *in vitro* and after 24 h incubation, the conditioned cell medium was harvested and used for ELV purification. An iodixanol density gradient based ultracentrifugation (UC) protocol was used **(Figure S1)** to obtain ELVs with a high purity with minimal protein contamination **(Figure S2)**[35] or residuals of commercial precipitation kit reagents.[36] After density gradient UC the fraction containing the ELVs was determined by immunoblotting against typical exosome-associated protein markers (HSP70, β-actin, CD63, CD81) on each fraction of the density gradient.[37] In this respect, fraction 5 contained the highest amount of exosomal markers. Moreover, the average density of this fraction was 1.14 g/ml which corresponds with earlier reports on the typical buoyant density of exosomes **(Figure 1A)**.[38] This fraction was used further for characterization and Raman spectroscopy experiments. As a ‘healthy‘ vesicle source, RBC were used as they are abundantly present in patient-derived blood samples. The same ELV purification protocol was used as described for the B16F10 melanoma cell-derived vesicles **(Figure S1)**.

After two additional washing steps by UC, the ELV pellet was suspended in ultrapure water (Millipore) and analyzed for size and zeta potential by single particle tracking analysis and dynamic light scattering, respectively. The majority of the B16F10 melanoma-derived ELVs had a hydrodynamic diameter of approx. 0.12 µm. RBC-derived vesicles were slightly larger with a size of approx. 0.17 µm **(Figure 1B)**. Both types of vesicles had a negative surface charge **(Figure 1B)**.

Finally, cryo-TEM was used as an additional confirmation of the presence of membranous structures in the purified samples **(Figure 1C)**.

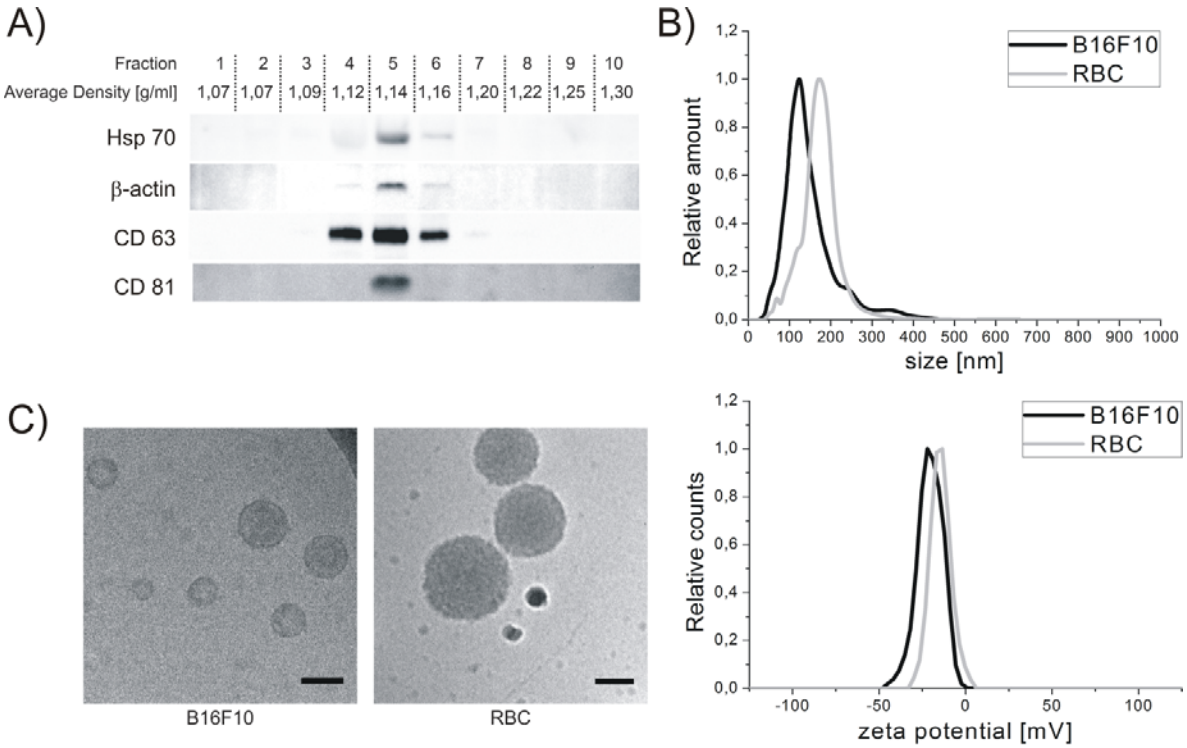

Figure 1. Characterization of purified B16F10 melanoma- and RBC-derived ELVs. A) Immunoblotting against exosomal markers HSP70, β-actin, CD63 and CD81 on the different density fractions after overnight density gradient UC of B16F10 melanoma derived conditioned medium. For each fraction the average density is reported [g/ml]. B) Representative size (upper) and zeta potential (lower) of B16F10 melanoma- (black) and RBC- (gray) derived ELVs determined by single particle tracking analysis and dynamic light scattering, respectively. C) Cryo-TEM images of B16F10 melanoma (left) and RBC-derived (right) ELVs. The scale bar indicates 100 nm.

2.2. Gold nanoparticle coating of ELVs

As a next step, we investigated if it would be possible to coat ELVs with AuNP while maintaining a colloidal single vesicle suspension. Specifically, we explored a coating strategy that is based on the electrostatic adsorption of cationic (due to a 4-dimethylaminopyridine (DMAP) coating), 10 nm AuNP **(Figure S3A and S3B)** onto the anionic surface of ELVs. AuNP were mixed with vesicles at increasing particle over vesicle ratios. It was observed that increasing the ratio of

AuNP:vesicles causes an initial increase in size (i.e. agglomeration) due to the zeta potential becoming more neutral. When increasing the ratio of AuNP:vesicles further, the zeta potential became strongly positive, resulting in a dispersion of individual AuNP coated ELVs, as confirmed by dynamic light scattering size measurements **(Figure 2A and 2B)** and cryo-TEM imaging **(Figure 2C and 2D)**. The latter also confirms the association between the negatively charged ELVs and the positively charged AuNP. Around 600 AuNP per B16F10 vesicle **(Figure 2A)** and 1200 AuNP per RBC vesicle **(Figure 2B)** were required to obtain a colloidal stable suspension. The fact that more AuNP per vesicles were needed to coat the RBC compared to the B16F10 melanoma vesicles is in accordance with the larger surface area of a RBC-derived vesicles. Moreover, these numbers approach the average theoretical amount of AuNP (i.e. 912 AuNP per B16F10- and 1291 AuNP per RBC-derived vesicle) needed to coat an entire vesicle in a monolayer as can be calculated from **Equation S1**. To obtain a SERS signal, AuNP need to be in close proximity to one another.[24] In this respect, high amounts of AuNP to vesicles were mixed (i.e. ~800 for B16F10 and ~1200 for RBC) for the SERS measurements. Indeed, for these higher ratios, cryo-TEM imaging showed nearly complete coating of both vesicle types with AuNP **(Figure 2C and 2D)**.

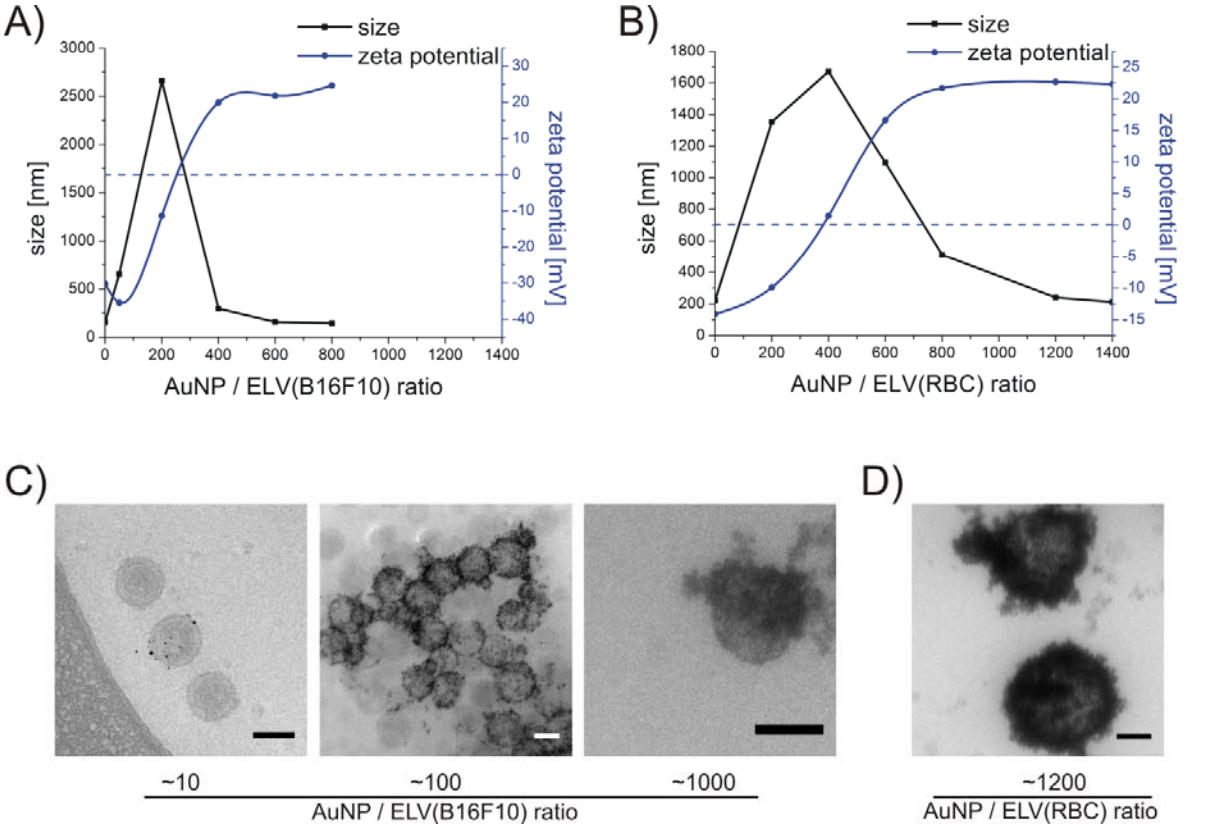

Figure 2. AuNP coating of ELVs. Average size and zeta potential of AuNP coated A) B16F10 melanoma-derived ELVs and B) RBC-derived ELVs, as a function of mounting AuNP:vesicle ratios. C) Cryo-TEM images of AuNP coated B16F10-derived ELVs. Mounting AuNP:vesicle ratios are indicated underneath the respective pictures. D) Cryo-TEM confirmation of full coating conditions for RBC-derived ELVs. The scale bars indicate 100 nm.

2.3. Recording SERS spectra of individual ELVs

Next, we investigated if this dense packing of AuNP on the vesicular surface indeed allows to generate a SERS spectral fingerprint. For these experiments we worked under high AuNP:vesicle ratios as described above. Spectra were recorded from individual AuNP coated ELVs adsorbed on a quartz surface **(Figure 3A)**. Peaks from (exosomal) biomolecules (green arrows) could be clearly identified in the spectra from B16F10 melanoma-derived vesicles **(Figure 3B)** and RBC-derived vesicles **(Figure 3C)**, apart from peaks arising from the DMAP coating of the AuNP (red arrows; cfr. **Figure S4**). **Table 1** gives an overview of the identified biomolecule peaks with their molecular origin. Most classes of biomolecules seem to be present, i.e. lipids, proteins, nucleic acids and

carbohydrates. It is of note that ELVs without AuNP coating could not generate a clear Raman signal under the same conditions, underscoring the importance of SERS for enhancing the signal of single vesicles.

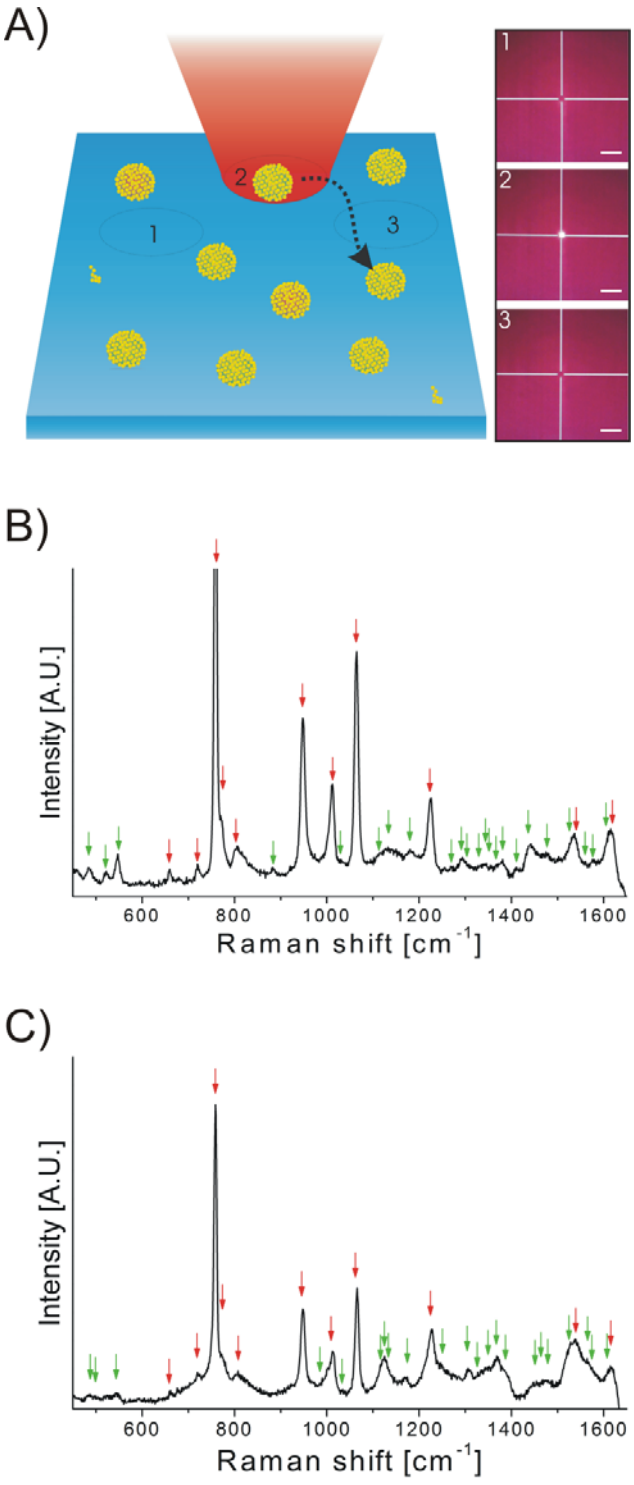

Figure 3. A) Schematic representation of the SERS measurements of AuNP coated ELVs. Each recorded spectrum is derived from another vesicle by moving the laser to a different spatial location (e.g. 1, 2, 3). The presence of a gold coated ELV was confirmed by a scattering signal (cfr. location 2). The scale bar indicates 10 μm. B) Representative, unmodified SERS spectrum of B16F10 melanoma-derived ELVs coated with AuNP and C) RBC-derived ELVs coated with AuNP. Red arrows indicate peaks arising from the DMAP AuNP coating. Green arrows indicate presumed ELV related peaks.

2.4. Identification of individual ELVs by spectral analysis

The obtained Raman spectra were subjected to two previously published dedicated statistical models: a Partial Least Square Discriminative Analysis (PLS-DA) and a Multivariate Curve Resolution Alternating Least Squares (MCR-ALS).[39, 40] Both models were trained and calibrated by Raman spectra obtained from pure samples i.e. AuNP alone, AuNP coated B16F10-derived vesicles and AuNP coated RBC-derived vesicles. The potential of Raman spectroscopy to discriminate between B16F10 melanoma and RBC-derived ELVs in an unbiased fashion was quantified by the PLS-DA model. A sensitivity of 95.8%, 88.0%, 95.1% and specificity of 95.5%, 95.4% and 98.0% for AuNP, B16F10 and RBC-derived ELVs, respectively was obtained **(Table 2)**. The here reported specificity and sensitivity of the model to discriminate among the different types of vesicles was assessed by cross-validation. Moreover, a parallel experiment was performed with a different Raman microscope allowing shorter acquisition times (500 ms compared to 10 s for the above measurements). Analysis of the obtained data was again performed using the PLS-DA model. The results show that the ability to separate between samples based on their SERS fingerprint was maintained **(Table S1)**.

Additionally, a MCR-ALS algorithm was applied on the obtained spectra **(Figure S5)**. Here it is important to note that the MCR-ALS model requires minimal constraints and prior information about the sample and is an unsupervised methodology. Nonetheless, the algorithm was able to deconvolve spectra **(Figure S5A)** which can be attributed (based on the score plots represented in **Figure S5B** and spectra in **Figure 3**) to: Quartz (surface), DMAP (AuNP coating), B16F10 and

RBC vesicles respectively. Indeed, this objectively shows the spectral discrepancy between ELVs from different origin.

2.5. Identification and quantification of B16F10 vesicles in a mixture with RBC-derived vesicles

Finally, to provide evidence of the diagnostic potential of this approach, mixtures of AuNP functionalized B16F10 cancerous- and RBC-derived ELVs were prepared at two different ratios. This setup more closely resembles the *in vivo* situation where cancerous vesicles need to be detected in patient samples containing a variety of vesicle types, especially highly abundant RBC-derived ELVs. To determine as a reference the exact ratio of both types of vesicles in the prepared mixtures, they were fluorescently labeled with lipophilic dyes (RBC ELVs = green; B16F10 ELVs = red) and subsequently coated with AuNP. The suspension was placed on a microscopy cover slip and confocal microscopy images were recorded. With in-house developed particle detection software the number of green and red fluorescent spots were counted **(Figure S6A)**. It was calculated that mixture 1 contained 51 ± 17 % cancerous ELVs and mixture 2 contained 15 ± 6% cancerous ELVs, respectively **(Figure S6B)**. From these images it could also be confirmed that the two types of AuNP coated vesicles did not agglomerate with one another as no co-localization of green and red spots could be seen.

Identical mixtures without fluorescent labels were subsequently prepared for SERS measurements. For each mixture between 60 and 80 spectra were recorded of AuNP coated vesicles. With the PLS-DA model each spectrum was assigned to one of the following groups: Unbound AuNP, RBC-derived ELVs or B1610-derived ELVs. In mixture 1 and 2, 38% and 6.3% cancerous vesicles were retrieved, respectively **(Figure 4)**. A few of the spectra were found to originate from unbound AuNP clusters **(Figure S7)**. These values reasonably correspond to the ratios as determined by

fluorescence microscopy and clearly demonstrate the potential of identifying and quantifying vesicles from different origins in a mixtures using SERS.

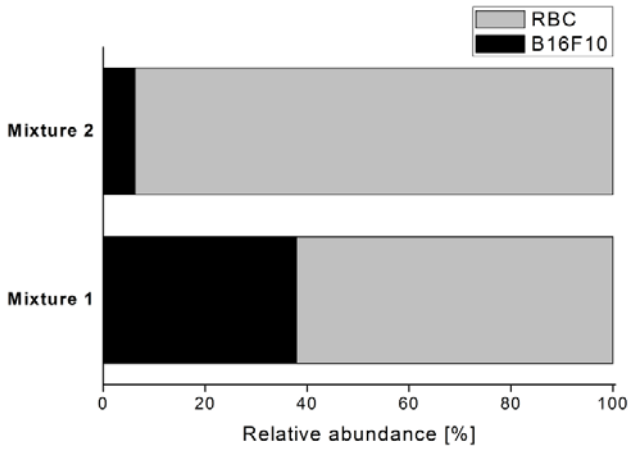

Figure 4. Composition of two ELV-mixtures determined by single vesicle SERS measurements in combination with PLS-DA statistical analysis. Mixture 1 and mixture 2 are two different blends of melanoma-derived and RBC-derived vesicles composed of 51% and 15% melanoma-derived vesicles, respectively. Each spectrum of an individual complex was allocated to one of three classes (unbound AuNP, AuNP coated B16F10 ELVs or AuNP coated RBC ELVs) by the PLS-DA model. Here the percentages B16F10- versus RBC-derived ELVs are reported for both mixtures.

3. Discussion

In this manuscript we investigated the possibility of identifying single ELVs by SERS. In contrast to previous diagnostic approaches, where the focus lies on detecting the presence or modified expression of a single exosomal component (i.e. a specific nucleic acid, lipid or protein)[41] using elaborate and time-consuming 'omics' studies, here the potential of SERS was tested to generate an optical fingerprint of individual ELVs coated with AuNP. If successful, such a method holds great potential for the identification of vesicles from different cellular origin in a quantitative manner from patient samples.

As an initial proof-of-concept, vesicles were purified from two distinct cell types. A skin-derived, B16F10 melanoma cell line was used as a model for carcinogenic cells and primary RBC as a model for healthy cells that are highly abundant in blood samples. To obtain vesicular concentrates as pure as possible, an iodixanol based density gradient UC protocol was used.[35] This is essential

as it was previously shown that residuals of commercial purification kits can interfere with the Raman fingerprint.[36] Moreover, other less stringent purification protocols (i.e. UC and commercial precipitation kits) suffer from limited purity due to co-purification of vesicle-independent proteins and nucleic acids, which might preclude the AuNP from interacting with the ELVs[42] and interfere with the Raman fingerprint.

In a next step, the purified vesicles were functionalized with ~10 nm AuNP to generate the SERS signal. The small diameter ensures that a large number of hot-spots are created in close proximity to the ELV-surface. The AuNP carry a cationic surface charge due to the DMAP coating which allows adsorption onto the anionic ELVs surface. Likely this association is charge based though it is also possible that the DMAP-molecules are exchanged for thiol-containing proteins present on the ELV surface.[43] Although aggregation was observed initially at low AuNP:vesicle ratios, at higher ratios a colloidal suspension of individual AuNP coated vesicles could be obtained. Indeed, once the overall surface charge of the AuNP coated ELVs became firmly positive (due to the DMAP coating), a mutual repulsion between the coated vesicles was created. This was confirmed using dynamic light scattering, cryo-electron microscopy and indirectly by confocal fluorescence microscopy. Additionally, as DMAP is a small molecule, the AuNP can reside in close proximity to the ELV surface. To the best of our knowledge this is the first time that single ELVs were enveloped with a gold coating. On average ~800 AuNP were used to coat the B16F10 melanoma vesicles, while ~1200 for RBC vesicles which is in agreement with the fact that RBC ELVs have a larger surface area and approaches the theoretical amount of AuNP to create a monolayer. This nanoshell of AuNP allowed to generate a SERS signal emanating from the ELVs due to a strong localized surface plasmon resonance between the closely packed AuNP present on the vesicular surface.[44]

The Raman peaks in the SERS spectra of single ELVs were found to arise in part from the DMAP and from ELV biomolecular components that are present in the vicinity of the AuNP. Biomolecular exosomal components were identified at 1123 cm^{-1} (lipids + proteins), 1172 cm^{-1} (proteins), 1307 cm^{-1} (proteins + lipids), 1366-1370 cm^{-1} (phospholipids + carbohydrates), 1445 cm^{-1} (lipids + proteins) and 1572-1576 cm^{-1} (nucleic acids). Interestingly, most of these pronounced peaks have previously been identified by others when recording Raman spectra of biological samples like erythrocytes[45] or even EVs (by classic Raman or SERS on bulk isolates).[18, 19, 32, 33, 36]

Next, we could show that the generated spectra, in combination with a PLS-DA classification model, allow us to separate between vesicles derived from B16F10 melanoma cells and RBC-derived vesicles. The fact that Raman spectroscopy is able to discriminate between vesicles from different cellular origin is in accordance with the very few reports available to date in which it was shown that classic Raman spectroscopy[18] and SERS[32, 33] on bulk or clusters of vesicles has discriminative power, even for more similar parent cells. Yet, as mentioned above, these reports are based on pure samples of one type of EV measured in bulk. Here, instead, we tackled the pending challenge of using SERS for the identification and quantification of single cancerous ELVs that are present in a mixture with 'healthy' RBC-derived vesicles. While future research should focus on testing more complex mixtures with multiple types of vesicles, still this is a promising proof-of-concept study. We consider the subtle difference discriminated by SERS in previous work on bulk EVs as a promising indication that detecting cancerous ELVs in complex mixtures would be possible with our single vesicle SERS approach.[28]

It is of note that an alternative approach with the potential of single vesicle SERS was very recently developed by Lee *et al.*. Their setup is based on Ag coated 'nanobowls' for hot-spot generation and SERS fingerprinting of EVs deposited into the nanobowls.[36] While a complex technological feat, our approach benefits from its simplicity and high-throughput potential. The AuNP based shell is

formed by simple self-assembly and AuNP functionalized ELVs can be measured by standard Raman equipment. Furthermore, our approach can be easily combined with (standard) microfluidics and an optical trapping unit allowing automated and fast SERS measurements. These characteristics will help to overcome the technological challenge of upscaling this technology for future clinical applications.

With the most sensitive set-up we could record clear Raman spectra at 0.5 s integration time per ELV. This means that per day it would be possible to analyze about 160.000 individual ELVs. As detectors continue to become more sensitive, and combined with the fact that a 0.5 s integration period already gave a strong and clear Raman spectrum, we expect that throughput could be increased 5-10 fold in the near future. Rapid recording of single spectra is indeed of pivotal importance for potential future diagnostic applications as 'diseased' ELVs are likely present in low abundance relative to the 'healthy' ones.

A particular challenge with our new approach is that SERS spectra of individual ELVs exhibit quite some variability, even for vesicles of the same parent cell. This originates from variability within the ELV population but potentially also from the (random) adsorption of AuNP on the vesicle surface and non-uniformity in hot spot generation.[46] In future research, therefore, it will be of interest to investigate other ways of functionalizing vesicles with AuNP with the aim to make the SERS spectra more uniform among vesicles of the same origin. This would allow to detect more subtle differences in molecular compositions and obtain more reliable molecular information from each individual vesicle. In turn this will lead to even better specificity and sensitivity. Apart from diagnostic applications, this method has the potential of being useful to deepen insight in molecular composition/diversity of the vesicles secreted by a certain cell type.[15]

4. Conclusion

Our findings show that applying SERS technology on AuNP-coated ELVs in combination with PLS-DA is capable of sensing biomolecular diversity between ELVs from different origins. Although future research should focus on more complex ELV mixtures, we have clearly demonstrated the potential of single vesicle identification by SERS to obtain ratios of vesicles from different origins in a mixture.

5. Experimental Section

Cell culturing and ELV purification

B16F10 melanoma cells (ATCC® CRL-6475™) were cultured in Dulbecco's Modified Eagle Medium (Invitrogen), supplemented with glutamine (2 mM), 10 % heat-inactivated fetal bovine serum (Hyclone), Sodium Pyruvate (1 mM), penicillin (100 U/mL) and streptomycin (100 µg/ml) (Invitrogen) at 37 °C in a humidified atmosphere containing 5 % CO_2. For the purification of ELVs, cells were first washed with phosphate-buffered saline (PBS, Invitrogen) and the cell medium was replaced with vesicle-depleted medium. The latter was prepared by ultrafiltration of complete cell culture medium through a 300 kDa filter (Millipore) using an Amicon stirred cell setup (Millipore) under three bar nitrogen pressure to remove bovine EVs. Cells were incubated for 24 hours after which the conditioned cell medium was harvested for vesicle purification.

Red blood cells (RBC) were isolated out of blood from a healthy volunteer as described previously[47] with minor modifications. Briefly, blood was collected in K_2EDTA coated tubes (Venosafe) and spun at 1 500 g for 15 minutes (Heraeus Multifuge 1S-R) within 10 minutes after blood collection. RBC were retained, washed twice and suspended in Ringer buffer (NaCl (150 mM), KCl (5 mM), $CaCl_2$ (2 mM), $MgCl_2$ (1mM), NaH_2PO_4 (2 mM), 4-(2-hydroxyethyl)-1-piperazineethanesulfonic acid (HEPES)-buffer (10 mM), Glucose (10 mM), pH=7.2) for 2 days at 37°C while shaking.

Vesicles derived from B16F10 melanoma cells and RBC were purified from conditioned cell medium or Ringer buffer, respectively by differential centrifugation followed by density gradient UC **(figure S1)**. First, conditioned cell medium/Ringer buffer was centrifuged for 10 minutes at 300 g and 10 minutes at 3 000 g. Next, the supernatant was concentrated by ultrafiltration using a 30 kDa filter (Millipore) in a Amicon stirred cell setup (Millipore) under nitrogen pressure. The concentrated sample was centrifuged (Beckman® L8-70M ultracentrifuge) at 10 000 g for 10 minutes using a SW55ti rotor (Beckman instruments) and the supernatant was placed on top of an iodixanol (Optiprep, Axis-Shield) based density gradient. The gradient was produced according to the manufacturer's instruction. Briefly, 1 ml of different iodixanol dilutions (12.5 %, 25 %, 37.5 % and 50 % in sucrose (250 mM), EDTA (1 mM), Tris-HCl (10 mM) buffer; pH = 7.4) were carefully laid underneath one another using a 21G needle. The samples were then centrifuged at 150 000 g for 15 hours. Next, the gradient was fractionated per 0.5 ml, diluted 10x in ultrapure water and centrifuged at 150 000 g for 150 minutes. Finally, the pellet was washed 1 more time and suspended in ultrapure water. The fraction containing the exosome associated proteins was used for further characterization and Raman spectroscopy experiments and the respective vesicles are referred to as ELVs.

Immunoblotting

In order to determine the density fraction containing the exosomes, pelleted vesicles from each fraction were resuspended in ice cold RIPA buffer (Sigma-Aldrich) mixed with MS-SAFE protease and phosphatase inhibitor cocktail (Sigma-Aldrich) and vortexed. Next, the samples were sonicated for 10 minutes and centrifuged at 13 000 g for 5 minutes. For protein separation, samples were diluted in 2x Laemmli buffer (Bio-Rad) with or without 5 % 2-mercaptoethanol (Sigma-Aldrich), heated at 95°C for 5 minutes and loaded on a 10 % mini-protean TGX precasted gel (Bio-Rad).

The polyacrylamide gel was ran at 100 V for 60 minutes in running buffer (Tris (25 mM) –Glycine (200 mM) – 0.1 % SDS). The blotting was done on an immunoblot PVDF 0.2 µm membrane (Bio-Rad) at 100 V for 90 minutes in blotting buffer (Tris (25 mM) –Glycine (200 mM) – 20 % Methanol – 0.05 % SDS). The blot was blocked for 1 hour using 3 % BSA, 0.1 % Tween20 (Sigma-Aldrich) in PBS buffer (Invitrogen). Next, primary antibodies were incubated overnight at 4°C on a shaker. After washing the blots with blocking buffer they were incubated with a secondary antibody conjugated to HRP for 1 hour at room temperature (Table S2). Visualization was done using the SuperSignal West Dura chemiluminscent kit (Thermo-Scientific) in combination with a VersaDocTM imaging system (Bio-Rad). All density fractions were loaded on one gel using equal volumes for objective comparison and the respective protein bands were cropped and aligned underneath one another for clarity.

DMAP coated AuNP

AuNP coated with DMAP were prepared as described by Gittins and Caruso.[48] Briefly, a $HAuCl_4$ aqueous solution was added to a tetraoctylammonium bromide in toluene solution under gentle stirring. Next, $NaBH_4$ was added to the mixture. After 30 minutes the toluene phase was separated from the aqueous phase and washed 3 times using H_2SO_4, NaOH and ultrapure water. Equal volumes of the AuNP in toluene solution and an aqueous DMAP solution were mixed and left to equilibrate for 1 hour. During this period the AuNP transfer from the organic toluene phase to the aqueous phase concomitantly exchanging the tetraoctylammonium bromide coat for a DMAP coating. Finally the aqueous phase, containing the AuNP coated with DMAP, is separated from the toluene phase. The final AuNP concentration was estimated by UV/VIS spectroscopy based on the optical density of the SPR-peak (Nanodrop 2000c; Thermo Scientific), assuming that the AuNP

are spherical with a molar extinction coefficient of 1.03 x10^8 $M^{-1}cm^{-1}$as calculated from **Equation 1** reported by Liu *et al.*.[49]

$$\ln(\varepsilon) = 3.3211 \times \ln(d) + 10.80505 \quad (1)$$

In which ε represents the molar extinction coefficient and d the diameter of the AuNP (10 nm).

AuNP coating of ELVs

ELVs were mixed with DMAP coated AuNP at different AuNP:vesicle ratios by mixing equal volumes using a pipette. After 10 minutes incubation at room temperature, the samples were diluted in ultrapure water/buffer and analyzed by different techniques (i.e. dynamic light scattering and cryo-TEM).

Concentration, size and zeta potential measurements

The concentration and size distribution of purified ELVs was determined by light scattering based single particle tracking using a NanoSight LM10 instrument (Malvern instruments Ltd.) equipped with a 405 nm laser. Prior to analysis, the concentrated vesicles were diluted in HEPES buffer (pH 7.4; 20 mM) to obtain a concentration in the range of 1.0 to 9.0 x 10^8 particles/ml to guarantee reliable measurements. Movies of 60 seconds were recorded and analyzed with the NTA Analytical Software version 2.3 (Malvern instruments Ltd.).

The size and zeta potential of ELVs and ELVs coated with AuNP (after dilution in HEPES-buffer) were measured by dynamic light scattering using a Zetasizer Nano ZS (Malvern instruments Ltd.), equipped with Dispersion Technology Software.

Cryo-transmission electron microscopy

Each ELV (with our without AuNP) sample (3.5 μL) was applied to a 300 mesh quantifoil grid and incubated for 30-60 seconds. Next, excess buffer was removed by blotting the grids for 3 seconds using a Whatmann 1 filter paper and the sample was snap frozen by plunging in liquid ethane at a temperature of -180°C and stored in liquid nitrogen until visualization. Next, the samples were transferred to a Gatan 914 cryoholder and imaged at low dose conditions at -177°C, using a JEOL JEM1400 TEM equipped with a 11 Mpxl Olympus SIS Quemesa camera.

Fluorescent labeling and confocal microscopy of ELVs

Purified B16F10- and RBC-derived vesicles were incubated for 15 minutes at 37°C with Vibrant DiD (Invitrogen) or PKH67 (Sigma), respectively (final dye concentration = 5 μM; in Diluent C (Sigma)). Next, non-incorporated dye and diluent C was removed using exosome spin columns (MWCO 3 000) pre-incubated with ultrapure water according to the manufacturer's instructions (Invitrogen).

The labeled ELVs were mixed with AuNP in the indicated ratios (cfr. SERS measurements) and visualized using a swept field confocal microscope (LiveScan SFC, Nikon Belux) equipped with a 60x oil immersion lens (NA = 1.4, Nikon). The ELVs were alternately irradiated with 488 nm and 647 nm laser light and images were recorded with an iXon Ultra EMCCD camera (Andor). Particle detection was done with in-house developed software in Matlab as previously described by Deschout *et al.*.[50] The ratio of B16F10 to RBC vesicles (B16F10:RBC ratio) was determined for each mixture by particle counting in at least 20 individual images at different spatial locations.

SERS measurements

ELVs (unlabeled) were mixed with DMAP coated AuNP at a fixed AuNP:vesicle ratio (i.e. ~800 for B16F10-derived ELVs and ~1200 for RBC-derived ELVs). Next, samples were diluted in

ultrapure water to ≤ 5 x 10^7 vesicles per µl to minimize the possibility that more than one vesicle is present in the focal detection volume. A droplet (60 µl) of the diluted sample was placed on a quartz substrate and SERS spectra were recorded using an inVia confocal Raman microscope (Renishaw, UK) equipped with a 60x WI lens (NA = 1, Nikon) and a 785 nm laser using a 10 second integration time and 15 mW power. Alternatively, a Raman microscope (Zeiss) equipped with a piezo-scanner (P500, physick instrumente) and a 785 nm laser focused through a 60x WI lens (NA = 1, Nikon) was used (integration time 500 ms). The spectra were acquired with a Spectra Pro500i (Acton Research) monochromator/spectrograph. The 785 nm laser was chosen to limit photodegradation and autofluorescence.[51, 52] All spectra were recorded at different locations in the sample. The presence of a gold coated ELV in the focal volume was confirmed by light scattering **(figure 3A)**.

Analysis of SERS spectra

For statistical analysis, the obtained spectra were pre-processed as described previously.[39] To assess the ability of Raman spectroscopy to discriminate RBC- and B16F10 melanoma-derived ELVs, PLS-DA was performed using the PLS toolbox from Eigenvector Research in MatLab. Cross-validation analysis was computed by Venetian blinds (10 splits and one sample per split). The number of retained latent variables was chosen to minimize the root mean square error of cross validation curves. Additionally, a MCR-ALS algorithm was used to analyze the spectra.

Supporting Information
Supporting Information is available from the Wiley Online Library or from the author.

Acknowledgements
SS and KR are doctoral and postdoctoral fellows respectively of the Research Foundation - Flanders (FWO). The support of this institution is gratefully acknowledged. AGS gratefully acknowledges the support of BOF (Ghent University), FWO, and FP-7 EU project “DINaMIT”.

PB acknowledges the support of the Hercules grant AKUL2011/30. MM and PL acknowledge the Laser Lab Europe (grant agreement no.284464, EC's Seventh Framework Programme), the Photonics4Life network of excellence, the European regional Development Fund, the MINECO Severo Ochoa grant (SEV-2015-0522) and thank the support of Fundació Cellex Barcelona. Part of the work has been conducted at the super resolution light microscopy and nanoscopy facility at ICFO. We also like to thank Dr. H. Moehwald from the MPI-KG (Germany) for the use of the Raman microscope.

Received: ((will be filled in by the editorial staff))
Revised: ((will be filled in by the editorial staff))
Published online: ((will be filled in by the editorial staff))

References

[1.] F. Properzi, M. Logozzi, S. Fais, *Biomarkers in medicine* **2013,** *7*, 769.

[2.] S. A. Melo, L. B. Luecke, C. Kahlert, A. F. Fernandez, S. T. Gammon, J. Kaye, V. S. LeBleu, E. A. Mittendorf, J. Weitz, N. Rahbari, C. Reissfelder, C. Pilarsky, M. F. Fraga, D. Piwnica-Worms, R. Kalluri, *Nature* **2015,** *523*, 177.

[3.] G. Raposo, W. Stoorvogel, *The Journal of cell biology* **2013,** *200*, 373.

[4.] R. M. Johnstone, A. Mathew, A. B. Mason, K. Teng, *Journal of cellular physiology* **1991,** *147*, 27.

[5.] M. S. Ostenfeld, D. K. Jeppesen, J. R. Laurberg, A. T. Boysen, J. B. Bramsen, B. Primdal-Bengtson, A. Hendrix, P. Lamy, F. Dagnaes-Hansen, M. H. Rasmussen, K. H. Bui, N. Fristrup, E. I. Christensen, I. Nordentoft, J. P. Morth, J. B. Jensen, J. S. Pedersen, M. Beck, D. Theodorescu, M. Borre, K. A. Howard, L. Dyrskjot, T. F. Orntoft, *Cancer research* **2014,** *74*, 5758.

[6.] H. Valadi, K. Ekstrom, A. Bossios, M. Sjostrand, J. J. Lee, J. O. Lotvall, *Nature cell biology* **2007,** *9*, 654.

[7.] H. Peinado, M. Aleckovic, S. Lavotshkin, I. Matei, B. Costa-Silva, G. Moreno-Bueno, M. Hergueta-Redondo, C. Williams, G. Garcia-Santos, C. Ghajar, A. Nitadori-Hoshino, C. Hoffman,

K. Badal, B. A. Garcia, M. K. Callahan, J. Yuan, V. R. Martins, J. Skog, R. N. Kaplan, M. S. Brady, J. D. Wolchok, P. B. Chapman, Y. Kang, J. Bromberg, D. Lyden, *Nature medicine* **2012,** *18*, 883.

[8.] D. Garnier, N. Jabado, J. Rak, *Proteomics* **2013,** *13*, 1595.

[9.] C. Lasser, V. S. Alikhani, K. Ekstrom, M. Eldh, P. T. Paredes, A. Bossios, M. Sjostrand, S. Gabrielsson, J. Lotvall, H. Valadi, *Journal of translational medicine* **2011,** *9*, 9.

[10.] M. Li, E. Zeringer, T. Barta, J. Schageman, A. Cheng, A. V. Vlassov, *Philos Trans R Soc Lond B Biol Sci* **2014,** *369*.

[11.] M. Szajnik, M. Derbis, M. Lach, P. Patalas, M. Michalak, H. Drzewiecka, D. Szpurek, A. Nowakowski, M. Spaczynski, W. Baranowski, T. L. Whiteside, *Gynecol Obstet (Sunnyvale)* **2013,** *Suppl 4*, 3.

[12.] D. S. Choi, J. Lee, G. Go, Y. K. Kim, Y. S. Gho, *Mol Diagn Ther* **2013,** *17*, 265.

[13.] H. Wang, L. Hou, A. Li, Y. Duan, H. Gao, X. Song, *Biomed Res Int* **2014,** *2014*, 864894.

[14.] J. Skog, T. Wurdinger, S. van Rijn, D. H. Meijer, L. Gainche, M. Sena-Esteves, W. T. Curry, Jr., B. S. Carter, A. M. Krichevsky, X. O. Breakefield, *Nature cell biology* **2008,** *10*, 1470.

[15.] M. Colombo, C. Moita, G. van Niel, J. Kowal, J. Vigneron, P. Benaroch, N. Manel, L. F. Moita, C. Thery, G. Raposo, *J Cell Sci* **2013,** *126*, 5553.

[16.] K. Laulagnier, H. Vincent-Schneider, S. Hamdi, C. Subra, D. Lankar, M. Record, *Blood cells, molecules & diseases* **2005,** *35*, 116.

[17.] J. R. Chevillet, Q. Kang, I. K. Ruf, H. A. Briggs, L. N. Vojtech, S. M. Hughes, H. H. Cheng, J. D. Arroyo, E. K. Meredith, E. N. Gallichotte, E. L. Pogosova-Agadjanyan, C. Morrissey, D. L. Stirewalt, F. Hladik, E. Y. Yu, C. S. Higano, M. Tewari, *Proc Natl Acad Sci U S A* **2014,** *111*, 14888.

[18.] I. Tatischeff, E. Larquet, J. M. Falcon-Perez, P. Y. Turpin, S. G. Kruglik, *Journal of extracellular vesicles* **2012,** *1*.

[19.] F. Lavialle, S. Deshayes, F. Gonnet, E. Larquet, S. G. Kruglik, N. Boisset, R. Daniel, A. Alfsen, I. Tatischeff, *Int J Pharm* **2009,** *380*, 206.

[20.] D. Graham, R. Goodacre, *Chem Soc Rev* **2008,** *37*, 883.

[21.] X. M. Qian, S. M. Nie, *Chem Soc Rev* **2008,** *37*, 912.

[22.] G. McNay, D. Eustace, W. E. Smith, K. Faulds, D. Graham, *Appl Spectrosc* **2011,** *65*, 825.

[23.] B. Sharma, R. R. Frontiera, A.-I. Henry, E. Ringe, R. P. Van Duyne, *Materials Today* **2012,** *15*, 16.

[24.] J. Langer, S. M. Novikov, L. M. Liz-Marzan, *Nanotechnology* **2015,** *26*, 322001.

[25.] S. D. Hudson, G. Chumanov, *Anal Bioanal Chem* **2009,** *394*, 679.

[26.] A. Yashchenok, A. Masic, D. Gorin, B. S. Shim, N. A. Kotov, P. Fratzl, H. Mohwald, A. Skirtach, *Small* **2013,** *9*, 351.

[27.] S. C. Luo, K. Sivashanmugan, J. D. Liao, C. K. Yao, H. C. Peng, *Biosensors & bioelectronics* **2014,** *61*, 232.

[28.] P. C. Wuytens, A. Z. Subramanian, W. H. De Vos, A. G. Skirtach, R. Baets, *Analyst* **2015,** *140*, 8080.

[29.] L. Mikoliunaite, R. D. Rodriguez, E. Sheremet, V. Kolchuzhin, J. Mehner, A. Ramanavicius, D. R. Zahn, *Scientific reports* **2015,** *5*, 13150.

[30.] T. Lemma, A. Saliniemi, V. Hynninen, V. P. Hytönen, J. J. Toppari, *Vibrational Spectroscopy* **2016,** *83*, 36.

[31.] T. Buchner, D. Drescher, H. Traub, P. Schrade, S. Bachmann, N. Jakubowski, J. Kneipp, *Analytical and bioanalytical chemistry* **2014,** *406*, 7003.

[32.] L. Tirinato, F. Gentile, D. Di Mascolo, M. L. Coluccio, G. Das, C. Liberale, S. A. Pullano, G. Perozziello, M. Francardi, A. Accardo, F. De Angelis, P. Candeloro, E. Di Fabrizio, *Microelectronic Engineering* **2012,** *97*, 337.

[33.] L. G. Laura T. Kerr, Karolina Weiner Gorzel, Shiva Sharma, Malcolm Kell, Amanda Mc Cann, Bryan M. Hennelly, *Biophotonics: Photonic Solutions for Better Health Care IV* **2014,** *91292Q*.

[34.] J. Lotvall, A. F. Hill, F. Hochberg, E. I. Buzas, D. Di Vizio, C. Gardiner, Y. S. Gho, I. V. Kurochkin, S. Mathivanan, P. Quesenberry, S. Sahoo, H. Tahara, M. H. Wauben, K. W. Witwer, C. Thery, *J Extracell Vesicles* **2014,** *3*, 26913.

[35.] J. Van Deun, P. Mestdagh, R. Sormunen, V. Cocquyt, K. Vermaelen, J. Vandesompele, M. Bracke, O. De Wever, A. Hendrix, *J Extracell Vesicles* **2014**.

[36.] C. Lee, R. P. Carney, S. Hazari, Z. J. Smith, A. Knudson, C. S. Robertson, K. S. Lam, S. Wachsmann-Hogiu, *Nanoscale* **2015,** *7*, 9290.

[37.] S. Mathivanan, C. J. Fahner, G. E. Reid, R. J. Simpson, *Nucleic acids research* **2012,** *40*, D1241.

[38.] D. M. Pegtel, L. Peferoen, S. Amor, *Philos Trans R Soc Lond B Biol Sci* **2014,** *369*.

[39.] M. Marro, C. Nieva, R. Sanz-Pamplona, A. Sierra, *Biochim Biophys Acta* **2014,** *1843*, 1785.

[40.] D. Ballabio, V. Consonni, *Analytical Methods* **2013,** *5*, 3790.

[41.] D. S. Choi, D. K. Kim, Y. K. Kim, Y. S. Gho, *Proteomics* **2013,** *13*, 1554.

[42.] A. Bonifacio, S. Dalla Marta, R. Spizzo, S. Cervo, A. Steffan, A. Colombatti, V. Sergo, *Analytical and bioanalytical chemistry* **2014,** *406*, 2355.

[43.] R. A. Sperling, W. J. Parak, *Philos Trans A Math Phys Eng Sci.* **2010,** *368*, 1333.

[44.] C. L. Haynes, R. P. Van Duyne, *The Journal of Physical Chemistry B* **2001,** *105*, 5599.

[45.] W. R. Premasiri, J. C. Lee, L. D. Ziegler, *The Journal of Physical Chemistry B* **2012,** *116*, 9376.

[46.] W. Xie, P. Qiu, C. Mao, *J Mater Chem* **2011,** *21*, 5190.

[47.] P. Vader, M. H. Fens, N. Sachini, B. A. van Oirschot, G. Andringa, A. C. Egberts, C. A. Gaillard, J. T. Rasmussen, R. van Wijk, W. W. van Solinge, R. M. Schiffelers, *Nanomedicine (Lond)* **2013,** *8*, 1127.

[48.] D. I. Gittins, F. Caruso, *Angew Chem Int Ed Engl* **2001,** *40*, 3001.

[49.] X. Liu, M. Atwater, J. Wang, Q. Huo, *Colloids Surf B Biointerfaces* **2007,** *58*, 3.

[50.] H. Deschout, T. Martens, D. Vercauteren, K. Remaut, J. Demeester, S. C. De Smedt, K. Neyts, K. Braeckmans, *Int J Mol Sci* **2013,** *14*, 16485.

[51.] K. G. Stamplecoskie, J. C. Scaiano, V. S. Tiwari, H. Anis, *The Journal of Physical Chemistry C* **2011,** *115*, 1403.

[52.] J. W. Kang, P. T. So, R. R. Dasari, D. K. Lim, *Nano letters* **2015,** *15*, 1766.

[53.] Z. Movasaghi, S. Rehman, I. U. Rehman, *Applied Spectroscopy Reviews* **2007,** *42*, 493.

Table 1. Enumeration and tentative assignment of SERS peaks for AuNP-coated B16F10 ELVs (B16F10_AuNP) and AuNP-coated RBC ELVs (RBC_AuNP).

Raman shift [cm^{-1}]	RBC_AuNP [a]	B16F10_AuNP [a]	Previously identified in EV isolates	Presumed origin[53] [b]
486	w	m		polysaccharide
521	w	m		S-S stretching (e.g. protein)
546	w	m		cholesterol
883		w	[18, 36]	$\rho(CH_2)$ (e.g. protein)
989	sh		[33]	
1032	w	sh	[18, 32]	CH_2CH_3 bending (e.g. phospholipid); v(C-C) (e.g. polysaccharide)
1115	sh	sh	[36]	C-O ribose (e.g. nucleic acid)
1124	s	m	[18, 19]	v_{22}(porphyrin half ring; typical for RBC) / C-C stretch (e.g. lipid, protein) / C-N (e.g. protein)
1134	sh	m	[32]	v(C-C) (e.g. lipid)
1172	m	sh	[36]	δ(C-H) (e.g. protein)
1179		m		v(C-C) or v(C-O) (e.g. phospholipids)
1243	sh		[18]	amide III (e.g. protein) / asymmetric phosphate stretching (e.g. nucleic acid)
1271		w	[18]	amide III (e.g. protein) / C=C (e.g. fatty acids)
1293		m	[19]	cytosine (nucleic acid) / CH_2 deformation (e.g. lipids)
1307	m	sh	[18, 33, 36]	C-N asymmetric stretching (e.g. protein) / CH_3CH_2 twisting (e.g. lipid)
1326	sh	sh	[36]	$\omega(CH_3CH_2)$ (e.g. nucleic acid)
1346	sh	w		
1354		w		guanine (nucleic acid)
1367	sh	sh		v(CH_3) (e.g. phospholipid)
1370	s	m		carbohydrate
1381	sh	m		δCH_3 symmetric (e.g. lipid)
1411		w		
1443	sh	s	[18, 19, 36]	$\delta(CH_2/CH_3)$ (e.g. protein, lipid)
1465	w		[36]	lipid
1477	w	w	[32]	DMAP + δ(C-H) (e.g. lipid, protein)
1528	w	sh	[18]	v(-C=C-) $_{conjugated}$
1563	sh	w		tryptophan
1576	w	w	[19]	guanine (nucleic acid)
1608	sh	sh	[18]	cytosine (nucleic acid) / phenylalanine (protein)

1618	s	s	[33]	DMAP/ν(C=C) (e.g. protein)

[a)]s: strong, m: medium, w: weak, sh: shoulder; [b)]ν: vibration, δ: deformation, ω: wagging, ρ: in plane rocking, DMAP: 4-dimethylaminopyridine

Table 2. PLS-DA classification of the spectra of pure samples (AuNP, B16F10 ELVs coated with AuNP and RBC ELVs coated with AuNP) .

Sample	n[a)]	PLS-DA prediction			
		Correct identification	Wrong identification	Sensitivity (%)	Specificity (%)
AuNP	24	24	0	100[b)] / 95.8[c)]	97.0[b)] / 95.5[c)]
B16F10_AuNP	25	23	2	92.0[b)] / 88.0[c)]	96.9[b)] / 95.4[c)]
RBC_AuNP	41	39	2	95.1[b)] / 95.1[c)]	100[b)] / 98.0[c)]

[a)]n is the amount of spectra recorded for each sample. Sensitivity and specificity were computed with[c)] and without[b)] cross validation.

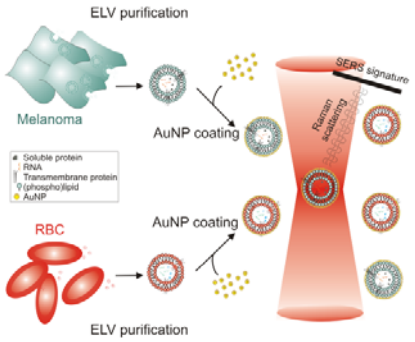

ToC. A method to obtain a surface enhanced Raman spectrum (SERS) of a single, nano-sized exosome-like vesicle (ELV) while maintaining individual ELVs in suspension. Based on these spectra ELVs derived from different cell types can be distinguished, hence allowing the identification and quantification of specific (cancerous) ELVs in a mixture.

Supporting Information

Identification of Individual Exosome-Like Vesicles by Surface Enhanced Raman Spectroscopy

*Stephan Stremersch, Monica Marro, Bat-El Pinchasik, Pieter Baatsen, An Hendrix, Stefaan C. De Smedt, Pablo Loza-Alvarez, Andre G. Skirtach, Koen Raemdonck, Kevin Braeckmans**

Supporting figures

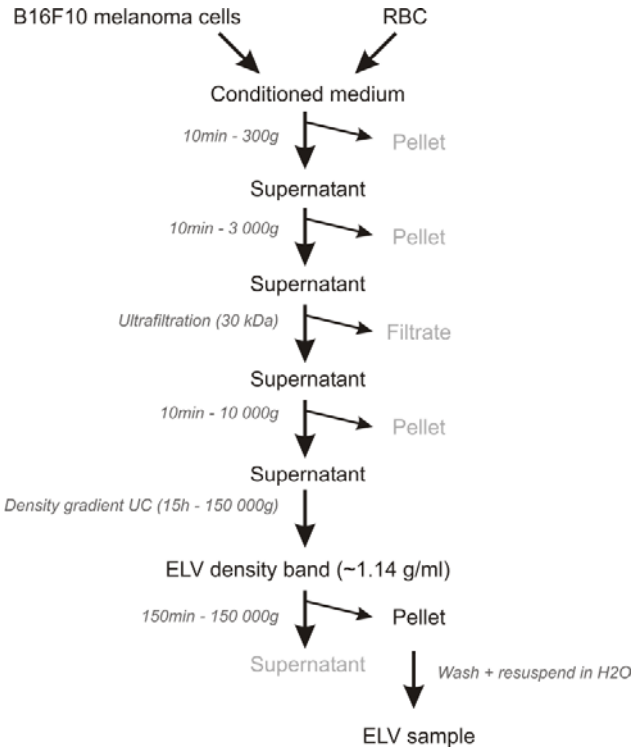

Figure S1. Schematic representation of the protocol used to purify exosome-like vesicles (ELVs) from conditioned cell medium.

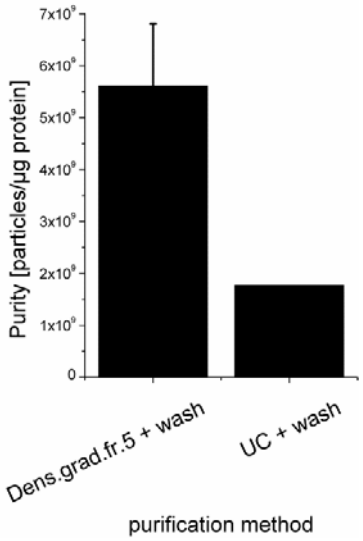

Figure S2. Comparison of the purity of B16F10-derived ELV isolations obtained by density gradient UC or UC alone, respectively. The purity is expressed as the amount of particles (determined by single particle tracking; NanoSight) per µg protein (determined by Pierce BCA protein assay kit; ThermoFisher Scientific) as recommended by Webber *et al*..[1]

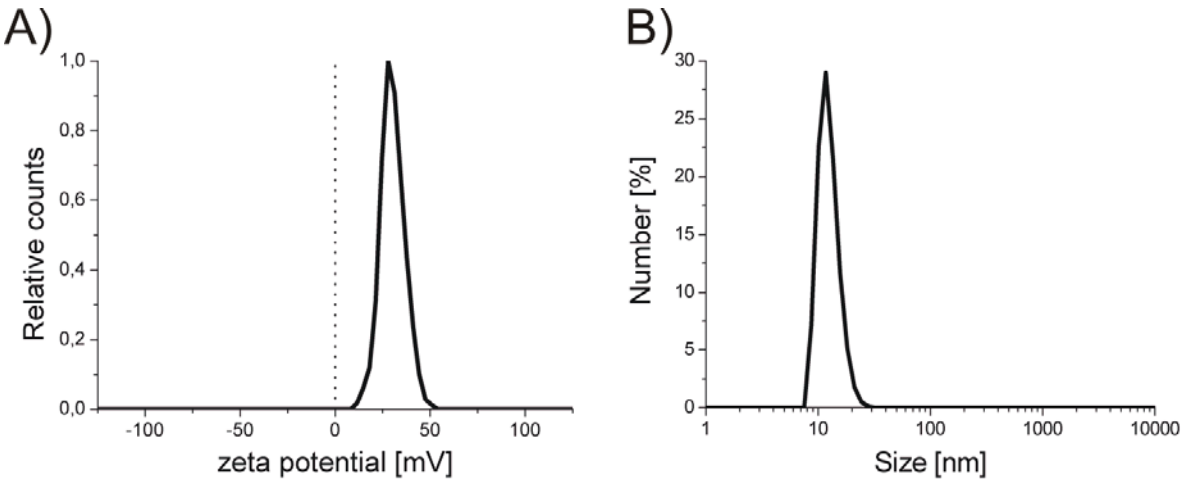

Figure S3. A) Zeta potential and B) hydrodynamic diameter of DMAP-coated gold nanoparticles, as determined by dynamic light scattering.

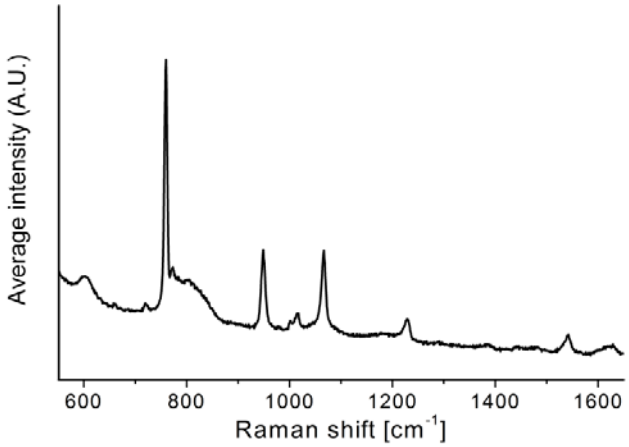

Figure S4. Average SERS spectrum of multiple normalized spectra (n>20) of DMAP-coated AuNP aggregates to determine the DMAP fingerprint.

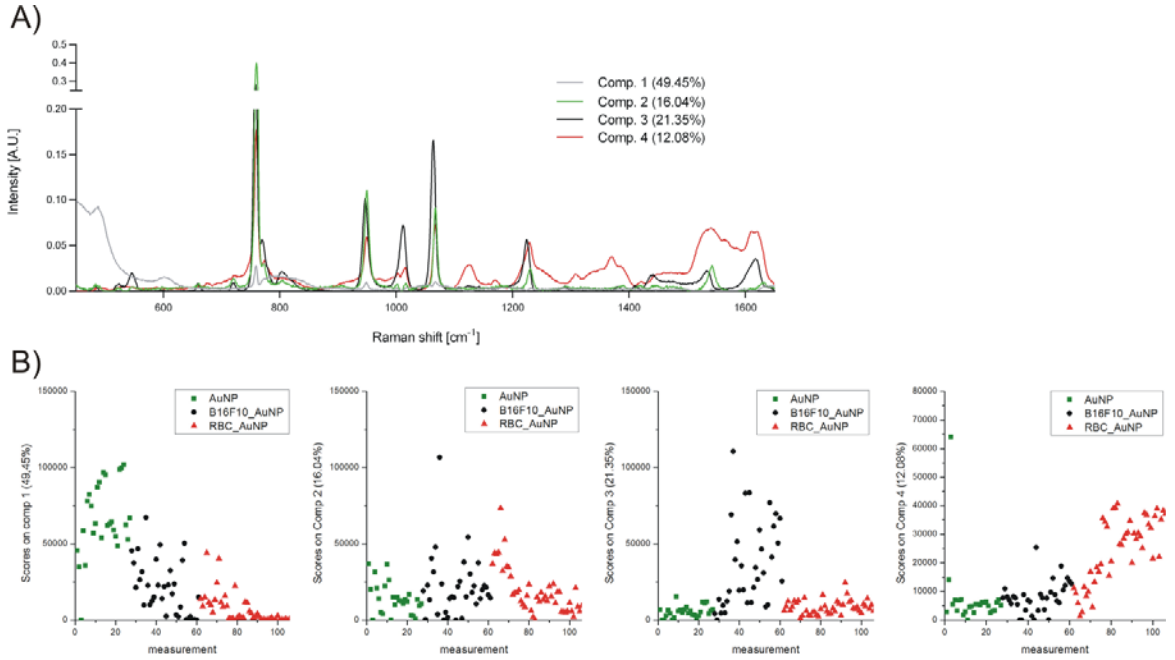

Figure S5. Output of the MCR-ALS algorithm. A) Deconvolved Raman spectra. B) Score for each deconvolved spectrum (y-axis) for all recorded spectra (x-axis) allowing to allocate the deconvolved spectra to a specific source (i.e. quartz, DMAP, B16F10 and RBC vesicles).

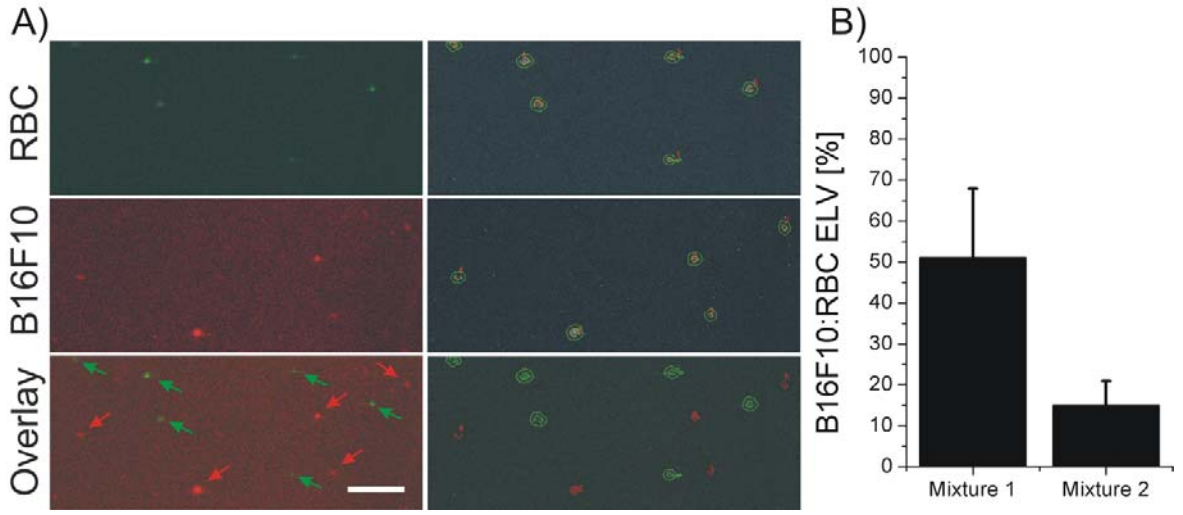

Figure S6. Mixtures of AuNP coated, fluorescently labeled RBC- (green) and B16F10 melanoma- (red) derived ELVs. A) A representative confocal image of mixture 1 (left) with particle location analysis (right). The scale bar indicates 20 µm. B) Percentage B16F10 melanoma-derived ELVs of the two B16F10:RBC mixtures based on fluorescence particle counting. Error bars indicate the standard deviation (*n*=20).

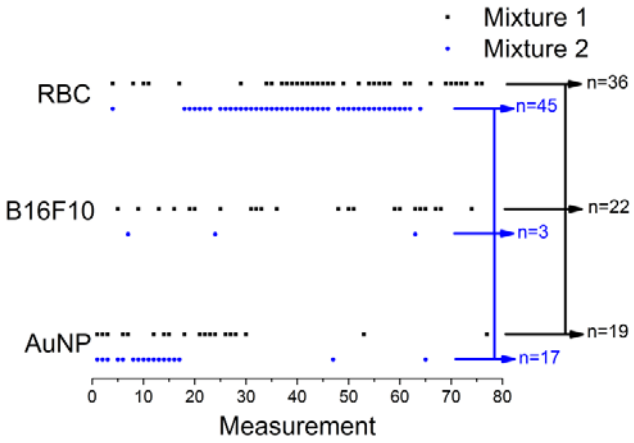

Figure S7. PLS-DA analysis of SERS measurements executed on two B16F10:RBC ELV mixtures. Each point represents an individual spectrum allocated to one of the three classes (unbound AuNP, AuNP coated B16F10 ELVs or AuNP coated RBC ELVs). *n* Represents the amount of spectra allocated to a specific class within a mixture. For the first mixture 77 spectra were recorded, For the second mixture 65 spectra were recorded.

Supporting tables

Table S1. PLS-DA classification of the spectra of pure samples recorded with an integration time of 500 ms.

Sample	*n* [a]	PLS-DA prediction	
		Correct identification	Wrong identification
B16F10_AuNP	53	53	0
RBC_AuNP	64	64	0

[a] *n* is the amount of spectra recorded for each sample

Table S2. Antibodies used for immunoblotting.

Target	Dilution	Supplier	Cat.#	Reducing conditions [b]	MW (kDa)
CD 81	1:1 000	LS biosciences Inc.	LS-C108453	No	~25-30
CD 63	1:500	Tebu-bio	GTX37555	No	~40
β-actin	1:1 000	Cell Signaling Techn.	4970	Yes	~45
Hsp 70	1:1 000	LS biosciences Inc.	LS-C24142	Yes	~70
Rabbit IgG[a]	1:50 000	Millipore	AP307P	N.A.	N.A.

[a] The secondary antibody is linked to a HRP-enzyme; [b] Reducing conditions imply heating of the sample to 95 °C for 5 minutes in the presence of 2-mercaptoethanol

Supporting equation

$$\frac{\overline{AuNP}}{ELV} = \frac{\sum_{i=1}^{n}\left[S_{ELV,i} \cdot \eta / SS_{AuNP}\right]}{n}$$

Equation S1. Equation used to calculate the theoretical average amount of AuNP needed to coat an entire vesicle surface in a monolayer, with *n* as the total amount of vesicles, $S_{ELV,i}$ as the surface of a vesicle i, η is the maximum packing density of a sphere which was fixed at 0.9 (hexagonal packing was assumed) and SS_{AuNP} as the surface of the section occupied by one AuNP. Calculations were based on the size distribution for each ELV type as depicted in figure 1B.

References

[1.] J. Webber, A. Clayton, Journal of extracellular vesicles 2013, 2.